Thermal Conductivity of Gaseous Dimethyl Ether from (263 to 383) K

Yugang Wang, Jiangtao Wu,* and Zhigang Liu

State Key Laboratory of Multiphase Flow in Power Engineering, Xi'an Jiaotong University, Xi'an, Shaanxi 710049, People's Republic of China

The thermal conductivity of gaseous dimethyl ether (DME) was measured over temperatures range from (263 to 383) K along 13 quasi-isotherms and at pressures up to saturation by the transient two hot-wire method. The standard uncertainty of the thermal conductivity of gaseous dimethyl ether is ± 1.0 %. The gaseous thermal conductivity was correlated as a function of pressure and temperature. The maximum deviation and the absolute mean deviation of measured data from the equations was −0.95 % and 0.36 %, respectively. The values for the thermal conductivity of the dilute gas and the saturated vapor were obtained by extrapolation.

Introduction

Dimethyl ether is an important chemical material and has many engineering applications such as assistant solvent, aerosol propellant, etc. In particular, it is regarded as an ideal potential clean fuel and an alternative refrigerant. Thus, it is urgent to obtain the thermophysical properties of dimethyl ether for such applications. Recently, some thermophysical properties of dimethyl ether including critical parameters, saturated densities, vapor pressure, surface tension, gas-phase PVT properties, viscosity, and thermal conductivity of the saturated liquid have been measured by our research group.[1−6] But there appear to be no measurements of the gaseous thermal conductivity of dimethyl ether in the literature. In this work, the thermal conductivities of gaseous dimethyl ether at temperatures from (263 to 383) K and at pressures up to 3300 kPa are reported.

Experimental Section

A transient two hot-wire apparatus developed recently by our group was used to measure the gaseous thermal conductivity of dimethyl ether. The transient hot-wire technique is widely recognized as the most accurate method for the measurement of the thermal conductivity of fluids. The fundamental working equation of the transient hot-wire method takes the form:[7]

$$\lambda(T_r, P) = (q/4\pi)(\mathrm{d}\Delta T_{id}/\mathrm{d}\ln t) \quad (1)$$

where q is the power input per unit length of wire, $\lambda(T_r, P)$ is the thermal conductivity of the fluid at a reference temperature (T_r) and at the working pressure (P), $\mathrm{d}\Delta T_{id}/\mathrm{d}\ln t$ is the slope of a line fit to the temperature rise in an ideal condition (ΔT_{id}) versus ln t data, where t represents the elapsed time. The ideal temperature rise is obtained by considering a number of corrections (δT_i) to the experimental temperature rise (ΔT_{exp}) according to

$$\Delta T_{id} = \Delta T_{exp} + \sum_i \delta T_i \quad (2)$$

The corrections $\sum \delta T_i$ have been described in refs 8, 9, and 10. In this work, the corrections concern mostly about the properties of wire. The reference temperature (T_r) associated with a given thermal conductivity data point is given by

$$T_r = T_0 + (\Delta T_1 + \Delta T_2)/2 \quad (3)$$

where T_0 is the initial temperature and ΔT_1 and ΔT_2 are the temperature rise at the start time and the end time of the linear region selected for the regression.

The schematic diagram of the transient hot-wire apparatus was shown in Figure 1. Two platinum wires which were of 15 μm in nominal diameter and (150 and 50) mm in length were used. A spring was used to ensure a constant tension on the platinum wire. The calibration of the resistance temperature relation of the platinum wire was carried out in the temperature range from (263 to 383) K. The maximum deviation and the absolute average deviation between the measured values and

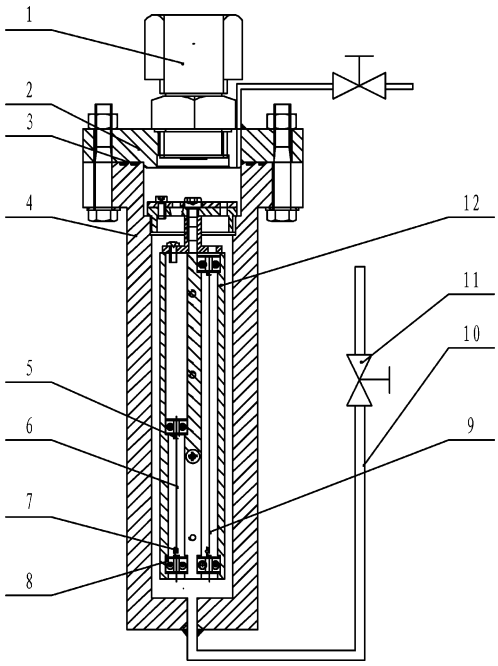

Figure 1. Hot-wire assembly: 1, conax seal; 2, flange; 3, Teflon seal; 4, pressure vessel; 5, gold terminal; 6, short wire; 7, weight/spring; 8, fastening component; 9, long wire; 10, pipeline; 11, valve; 12, cell.

* Corresponding author. E-mail: jtwu@mail.xjtu.edu.cn. Fax: +86-29-82668789.

10.1021/je050305z CCC: $33.50
Published on Web 10/28/2005

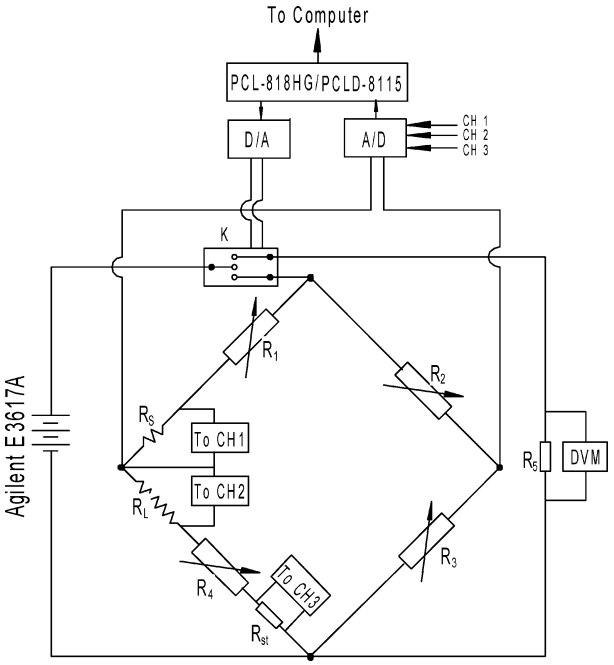

Figure 2. Circuit diagram for the transient hot-wire apparatus.

Table 1. Experimental Data of the Thermal Conductivity of Nitrogen

T_r	P	λ_{exp}	λ_{eq}	$100(\lambda_{exp} - \lambda_{eq})$	q
K	kPa	mW·m^{-1}·K^{-1}	mW·m^{-1}·K^{-1}	λ_{eq}	mW·m^{-1}
235.41	3405.4	23.34	23.22	0.51	72.23
235.72	3405.4	23.33	23.24	0.39	82.18
255.70	1281.1	23.32	23.29	0.11	72.81
256.26	1281.1	23.23	23.33	−0.44	88.10
255.55	5432.8	26.00	25.87	0.49	88.60
255.86	5432.8	25.96	25.89	0.27	100.66
275.41	1027.7	24.41	24.54	−0.51	66.81
276.11	1027.7	24.35	24.58	−0.94	86.67
275.39	5057.3	26.74	26.74	0.01	83.28
276.05	5057.3	26.90	26.77	0.47	109.43
295.15	1844.1	26.06	26.20	−0.53	73.10
295.68	1844.1	25.99	26.23	−0.93	86.25
295.25	4380.8	27.31	27.49	−0.65	83.47
295.92	4380.8	27.38	27.53	−0.54	110.13
325.32	716.0	27.58	27.72	−0.49	68.35
326.39	716.0	27.63	27.79	−0.56	101.75
325.43	2042.9	28.42	28.21	0.73	85.21
326.20	2042.9	28.45	28.26	0.67	104.59
326.23	4941.8	29.61	29.59	0.08	121.37

the correlated equation were 0.1 % and 0.05 %, respectively. The apparatus and connections were all made of stainless steel (1Cr18Ni9Ti), and the total volume was about 180 mL.

The circuit diagram used was shown in Figure 2. It consists of several components: a Wheatstone bridge, an Advantech PCL-818HG high-precision DAQ card, a high-speed analogue switch (model: MAX303), an Agilent E3617A DC power supply, and an industrial computer. The Wheatstone bridge included four high-accuracy DC decade resistance boxes (uncertainty 0.01 %, minimum step 0.001 Ω), a 10 Ω standard resistor (uncertainty 0.002 %), and the two wires in opposing legs of the bridge. The bridge imbalance was measured by the Advantech PCL-818HG with the range (0 to 10) mV (uncertainty 0.08 %) at a frequency of 1000 Hz.

The transient hot-wire apparatus was immersed completely in a thermostatic bath. The methyl silicon oil was selected as the bath fluid for the temperature range from (243 to 403) K. The temperature stability of the thermostatic bath was better

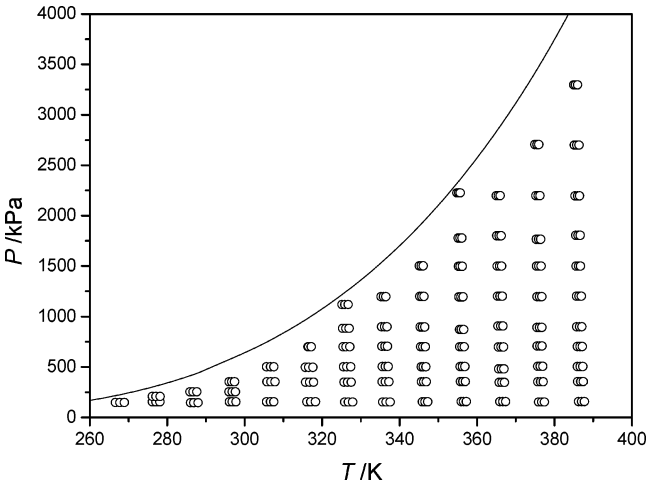

Figure 3. Temperature and pressure ranges for the experimental points: ○, measured state point; −, saturated vapor pressure.

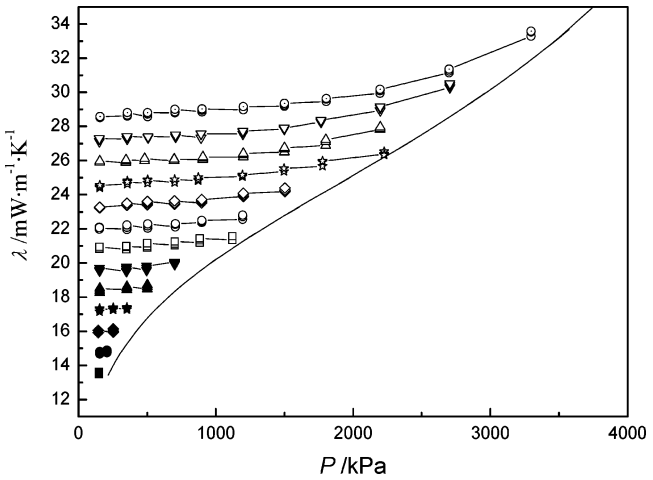

Figure 4. Thermal conductivity of gaseous dimethyl ether vs pressure near different isotherms: ■, 263.15 K; ●, 273.15 K; ◆, 283.15 K; ★, 293.15 K; ▲, 303.15 K; ▼, 313.15 K; □, 323.15 K; ○, 333.15 K; ◇, 343.15 K; ☆, 353.15 K; △, 363.15 K; ▽, 373.15 K; ◎, 383.15 K.

than ± 4 mK·h^{-1}. The temperature was measured with an ASL F18 AC thermometry bridge and a 25.5 Ω standard platinum resistance thermometer. The total uncertainty of temperature for thermal conductivity was less than ± 10 mK (ITS-90) with a coverage factor of $k = 2$. For pressure measurement, a high-precision quartz pressure sensor (Paroscientific Inc., model 42K-101) and a differential pressure transducer (Rosemount, model 3051) were used. The measurement range of pressure was from (0 to 13.8) MPa. The uncertainties of the pressure sensor and the pressure transducer were 0.01 % and 0.075 %, respectively. The total uncertainty of pressure for thermal conductivity was less than ± 1.5 kPa. The details about the thermostatic bath, temperature measurement, and pressure measurement have been given in previous papers.[6,11]

The total uncertainty of the experimental thermal conductivity obtained with the transient hot-wire method was estimated as follows.[12] The length of the platinum wires was measured by a cathetometer, and $\delta L/L$ was known to ± 0.04 % and ± 0.015 % for the short and long wire, respectively. The uncertainty in the temperature coefficient of the platinum wire was estimated to be within ± 0.1 %, the uncertainty in the heat generation of the hot wire was less than ± 0.1 %, and the uncertainty in the temperature-rise slope $d\Delta T/d \ln t$ of the hot wire was less than

Table 2. Experimental Data of the Thermal Conductivity of Gaseous Dimethyl Ether

T_r	P	λ_{exp}	q	T_r	P	λ_{exp}	q	T_r	P	λ_{exp}	q	T_r	P	λ_{exp}	q
K	kPa	mW·m^{-1}·K^{-1}	mW·m^{-1}	K	kPa	mW·m^{-1}·K^{-1}	mW·m^{-1}	K	kPa	mW·m^{-1}·K^{-1}	mW·m^{-1}	K	kPa	mW·m^{-1}·K^{-1}	mW·m^{-1}
266.62	148.1	13.48	55.65	326.20	701.6	21.13	78.20	356.86	504.3	24.85	102.74	375.54	707.6	27.38	76.18
267.77	148.1	13.59	72.87	327.16	701.6	21.25	102.78	355.55	701.6	24.72	68.47	376.22	707.6	27.49	98.91
268.94	148.1	13.63	90.79	325.31	883.7	21.19	58.02	356.10	701.6	24.89	84.34	376.81	707.6	27.51	117.83
276.20	155.8	14.68	53.92	326.11	883.7	21.33	78.92	356.72	701.6	24.90	102.60	375.46	892.8	27.33	76.09
277.12	155.8	14.76	69.99	326.99	883.7	21.45	102.25	355.47	872.5	24.83	68.47	376.14	892.8	27.56	98.82
278.14	155.8	14.82	87.56	325.16	1120.2	21.35	57.99	355.97	872.5	24.89	84.23	376.72	892.8	27.58	117.89
276.20	207.5	14.75	55.12	325.88	1120.2	21.35	78.86	356.57	872.5	25.02	102.35	375.49	1198.6	27.56	81.33
277.09	207.5	14.83	70.69	326.73	1120.2	21.56	103.01	355.33	1194.9	25.06	68.38	376.17	1198.6	27.70	104.70
278.17	207.5	14.89	89.62	335.66	152.2	21.98	56.46	355.82	1194.9	25.08	84.25	376.75	1198.6	27.73	124.93
286.05	144.6	15.92	53.80	336.55	152.2	22.11	76.78	356.38	1194.9	25.16	102.33	375.36	1499.6	27.84	81.23
286.89	144.6	16.05	68.03	337.54	152.2	22.07	99.69	355.20	1497.3	25.36	68.43	375.97	1499.6	27.93	105.33
287.99	144.6	16.06	87.75	335.48	353.4	21.97	56.46	355.69	1497.3	25.53	85.02	376.56	1499.6	27.91	124.88
285.91	253.2	15.94	58.80	336.32	353.4	22.09	76.75	356.21	1497.3	25.54	102.52	375.29	1766.8	28.26	81.35
286.67	253.2	16.00	68.05	337.25	353.4	22.23	99.64	355.11	1777.8	25.67	68.52	375.92	1766.8	28.31	104.76
287.68	253.2	16.14	87.28	335.54	505.2	22.04	60.91	355.58	1777.8	25.92	85.04	376.46	1766.8	28.37	125.08
296.03	154.5	17.15	56.82	336.37	505.2	22.17	81.98	356.09	1777.8	25.97	102.57	375.17	2197.8	28.93	81.25
296.80	154.5	17.28	71.82	337.06	505.2	22.29	99.55	354.82	2226.0	26.37	68.21	375.76	2197.8	29.10	104.62
297.76	154.5	17.34	90.32	335.43	705.2	22.12	60.91	355.22	2226.0	26.53	84.04	376.28	2197.8	29.17	124.98
295.96	253.2	17.25	56.59	336.23	705.2	22.26	81.97	355.66	2226.0	26.32	102.13	374.95	2704.4	30.29	81.19
296.76	253.2	17.33	72.69	336.91	705.2	22.31	100.27	365.86	156.4	25.96	71.98	375.49	2704.4	30.41	104.58
297.64	253.2	17.39	90.10	335.35	898.7	22.38	60.92	366.66	156.4	25.91	93.56	375.95	2704.4	30.51	124.87
296.02	352.9	17.26	61.96	336.11	898.7	22.44	82.02	367.38	156.4	25.97	112.58	386.20	156.6	28.52	90.04
296.69	352.9	17.36	75.96	336.74	898.7	22.50	99.56	365.68	346.3	25.89	72.00	387.03	156.6	28.58	114.61
297.39	352.9	17.40	90.59	335.18	1196.9	22.56	60.89	366.42	346.3	25.97	93.46	387.74	156.6	28.59	135.59
305.64	155.2	18.27	57.72	335.88	1196.9	22.72	81.92	367.09	346.3	26.04	112.61	386.01	355.6	28.61	90.08
306.69	155.2	18.39	77.09	336.45	1196.9	22.80	99.53	365.59	481.6	26.00	72.07	386.79	355.6	28.67	114.61
307.53	155.2	18.52	100.75	345.88	154.3	23.22	65.04	366.31	481.6	25.99	93.56	387.44	355.6	28.81	135.57
305.80	352.8	18.42	57.73	346.52	154.3	23.24	80.56	366.96	481.6	26.12	112.76	385.93	503.9	28.57	90.87
306.80	352.8	18.54	79.09	347.27	154.3	23.27	98.51	365.51	697.2	25.98	72.10	386.65	503.9	28.73	114.80
307.82	352.8	18.61	100.75	345.67	352.7	23.38	64.91	366.20	697.2	26.09	93.67	387.32	503.9	28.81	135.69
305.64	502.4	18.48	58.39	346.26	352.7	23.40	80.37	366.82	697.2	26.08	112.76	385.95	703.0	28.80	90.87
306.69	502.4	18.61	81.95	346.93	352.7	23.50	97.80	365.42	906.2	26.06	72.09	386.60	703.0	28.86	115.57
307.53	502.4	18.72	100.77	345.57	502.5	23.41	64.90	366.10	906.2	26.15	93.76	387.21	703.0	29.01	135.69
316.05	153.9	19.55	59.36	346.15	502.5	23.51	80.44	366.70	906.2	26.22	112.78	385.77	899.9	28.85	90.22
317.06	153.9	19.57	80.02	346.82	502.5	23.61	98.41	365.30	1202.0	26.22	72.04	386.48	899.9	28.95	114.84
318.26	153.9	19.71	104.64	345.47	700.0	23.44	64.81	365.94	1202.0	26.35	93.76	387.08	899.9	29.03	135.31
315.77	348.9	19.52	58.79	346.03	700.0	23.50	80.36	366.52	1202.0	26.42	112.78	385.66	1201.3	28.97	90.86
316.75	348.9	19.67	80.73	346.64	700.0	23.64	97.62	365.20	1500.1	26.50	72.04	386.33	1201.3	29.17	114.78
317.81	348.9	19.77	104.69	345.35	897.3	23.52	64.84	365.81	1500.1	26.69	93.63	386.93	1201.3	29.16	135.88
315.68	496.3	19.58	59.48	345.90	897.3	23.63	80.30	366.35	1500.1	26.75	112.72	385.56	1500.6	29.19	90.17
316.55	496.3	19.71	80.20	346.49	897.3	23.72	97.56	365.09	1801.9	26.89	71.43	386.22	1500.6	29.26	114.84
317.63	496.3	19.83	105.61	345.23	1200.4	23.90	64.84	365.70	1801.9	27.10	93.58	386.74	1500.6	29.36	135.80
316.35	700.4	20.06	80.20	345.74	1200.4	23.99	80.39	366.23	1801.9	27.23	112.71	385.48	1805.7	29.46	90.84
316.56	700.4	19.92	84.95	346.29	1200.4	24.08	97.74	364.94	2198.1	27.82	71.90	386.13	1805.7	29.59	115.53
317.20	700.4	19.99	101.03	345.11	1503.9	24.18	64.95	365.51	2198.1	27.89	93.50	386.65	1805.7	29.64	135.77
325.83	151.5	20.82	57.61	345.59	1503.9	24.27	80.44	365.99	2198.1	27.96	112.72	385.35	2197.0	29.95	90.15
326.79	151.5	20.87	78.37	346.12	1503.9	24.40	97.78	375.90	152.4	27.13	76.19	385.98	2197.0	30.10	114.75
327.88	151.5	20.94	102.51	355.89	156.1	24.41	68.64	376.68	152.4	27.26	98.24	386.50	2197.0	30.17	135.78
325.64	348.0	20.80	58.03	356.52	156.1	24.47	84.67	377.40	152.4	27.30	118.24	385.16	2700.7	31.15	90.16
326.53	348.0	20.93	78.95	357.23	156.1	24.56	102.81	375.72	354.0	27.27	76.14	385.74	2700.7	31.26	114.09
327.53	348.0	20.98	102.44	355.74	356.1	24.62	68.59	376.45	354.0	27.39	98.90	386.38	2700.7	31.36	143.30
325.53	500.8	20.91	58.06	356.31	356.1	24.81	84.54	377.08	354.0	27.42	117.88	384.94	3297.7	33.29	90.85
326.36	500.8	21.00	78.30	356.98	356.1	24.75	102.74	375.63	507.4	27.34	76.14	385.44	3297.7	33.54	114.80
327.38	500.8	21.16	103.10	355.64	504.3	24.68	68.59	376.35	507.4	27.37	98.88	386.00	3297.7	33.58	143.27
325.41	701.6	21.04	57.95	356.20	504.3	24.88	84.54	376.96	507.4	27.40	117.87				

± 0.2 %. Accounting for the uncertainty in the deviations from the mathematical ideal model and the uncertainty in the presence of other modes of heat transfer, which were reduced to a small magnitude for the properly designed instrument and the well-chosen operating conditions, the overall standard uncertainty of the present thermal conductivity measurements was estimated to be better than ± 1.0 %.

Before the apparatus was used to measure the thermal conductivity of gaseous dimethyl ether, the performance of the apparatus was checked by measuring the thermal conductivity of nitrogen. The mass fraction purity of the sample provided by Messer was better than 99.9995 %. The measurement results of thermal conductivity of nitrogen were listed in Table 1. Compared to the calculated values of thermal conductivity of nitrogen from REFPROP 7.0,[13] the maximum deviation was less than 1.0 %, and the mean deviation was 0.49 %. The comparisons indicated that the measurement uncertainty of the thermal conductivity was better than ± 1.0 %.

Results and Analysis

The sample of dimethyl ether was provided by Zhongshan Fine Chemical Co., Ltd. The mass fraction purity was better than 99.95 %, as indicated by analysis with gas chromatograph (made by Agilent Technologies, model: 6890N). A flame ionization detector (FID) and a capillary column (GS-GASPRO, model Agilent 113-4362) were used for the analysis with the carrier hydrogen at 4.0 mL/min, and the oven temperature and the detector temperature are 423 K and 473 K, respectively. Hence, the sample was not purified further.

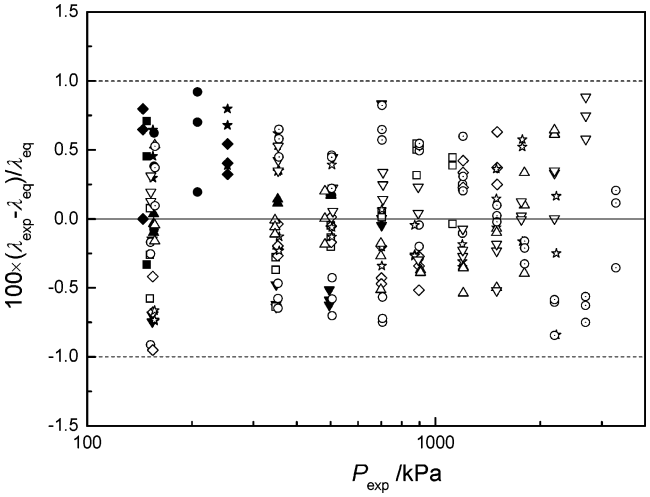

Figure 5. Relative deviations of the experimental thermal conductivity data from eq 4 (plotted vs pressure): ■, 263.15 K; ●, 273.15 K; ◆, 283.15 K; ★, 293.15 K; ▲, 303.31 K; ▼, 313.15 K; □, 323.15 K; ○, 333.15 K; ◇, 343.15 K; ☆, 353.15 K; △, 363.15 K; ▽, 373.15 K; ◎, 383.15 K.

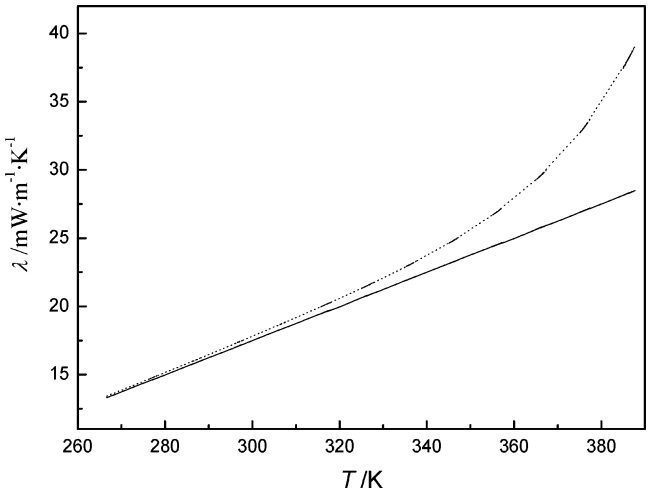

Figure 6. Thermal conductivity of the saturation vapor and the ideal gas of dimethyl ether: —, dilute gas; - - -, saturated vapor.

Table 3. Coefficients Used in Equations 4, 5, and 6

coefficient	value	coefficient	value
a_0/d_0	-2.009408×10^{1}	c_0	8.595429×10^{3}
a_1/d_1	1.252783×10^{-1}	c_1	-1.693336×10^{2}
b_1	5.386311×10^{-4}	c_2	1.389870
b_2	-1.545606×10^{-7}	c_3	-6.086694×10^{-3}
b_3	1.589597×10^{-10}	c_4	1.501719×10^{-5}
b_4	$-4.382642 \times 10\text{-}^{15}$	c_5	-1.980038×10^{-8}
		c_6	1.090623×10^{-11}

The thermal conductivity of gaseous dimethyl ether was measured at temperatures ranging from (263 to 383) K and at pressures up to saturation. The maximum pressure was 3300 kPa. Totally 77 data points were obtained along 13 quasi-isotherms, and the distribution in the temperature−pressure diagram is shown in Figure 3 where the saturated vapor pressures were from ref 2. The results are listed in Table 2 and illustrated in Figure 4. The λ_{exp} values represented here are the averages of several runs at the same heat power, whose repeatability at the same temperature and pressure was better than ± 0.5 %.

Usually, the thermal conductivity of gas is correlated as the function of temperature and density. But only a limited number of gaseous PVT data of dimethyl ether have been reported.[6] Hence, in this work, the experimental values of the thermal conductivity of gaseous dimethyl ether were correlated as the function of temperature and pressure using a least-squares method to the following equation:

$$\lambda/\mathrm{mW{\cdot}m^{-1}{\cdot}K^{-1}} = a_0 + a_1(T/\mathrm{K}) + \sum_{i=1}^{4} b_i (P/\mathrm{kPa})^i \qquad (4)$$

and the coefficients are listed in Table 3. The deviations between the experimental and calculated values are shown in Figure 5, where they are plotted as a function of pressure. The maximum deviation and the mean deviation of experimental data from eq 4 are −0.95 % and 0.36 %, respectively.

In practical applications, the thermal conductivities for the saturation vapor as well as for the dilute gas ($\rho \rightarrow 0$ or $P \rightarrow 0$) are of special interest. Therefore, the thermal conductivity for saturated vapor and for dilute gas, indicated by λ_s and λ_0, respectively, are correlated by

$$\lambda_s/\mathrm{mW{\cdot}m^{-1}{\cdot}K^{-1}} = \sum_{i=0}^{6} c_i (T/\mathrm{K})^i \qquad (5)$$

$$\lambda_0/\mathrm{mW{\cdot}m^{-1}{\cdot}K^{-1}} = d_0 + d_1(T/\mathrm{K}) \qquad (6)$$

where the coefficients are also listed in Table 3. Considering that the upper-limit pressure is very close to the saturated pressure that was measured with high accuracy,[2] and the lower-limit pressure is 150 kPa, the uncertainty of the extrapolated thermal conductivity of saturated vapor and dilute gas should be close to that of the measurements and could be regarded as ±1.0 % in this work. The applicable temperature range of eq 4 and eq 5 is from (263 to 383) K. Finally, the thermal conductivity for saturated vapor and for dilute gas is plotted as a function of temperature in Figure 6.

Conclusion

Using a transient hot-wire apparatus whose performance was checked with nitrogen, the thermal conductivity of gaseous dimethyl ether was measured in the temperature range from (263 to 383) K along 13 quasi-isotherms and at pressures up to 3300 kPa. The uncertainty of the results is ±1.0 %. The measured data were correlated as a function of temperature and pressure with the mean deviation of 0.36 % and a maximum deviation of −0.95 %. For practical applications, the equations for saturated gas and dilute gas were also derived.

Literature Cited

(1) Wu, J. T.; Liu, Z. G.; Wang, B.; Pan, J. Measurements of critical parameters and saturated densities of dimethyl ether. *J. Chem. Eng. Data* **2004**, *49*, 704−708.
(2) Wu, J. T.; Liu, Z. G.; Pan, J.; Zhao, X. M. Vapor pressure measurements of dimethyl ether from (233 to 399) K. *J. Chem. Eng. Data* **2004**, *49*, 32−34.
(3) Wu, J. T.; Liu, Z. G.; Wang, F. K.; Ren, C. Surface tension of dimethyl ether from (213 to 368) K. *J. Chem. Eng. Data* **2003**, *48*, 1571−1573.
(4) Wu, J. T.; Liu, Z. G.; Bi, S. S.; Meng, X. Y. Viscosity of saturated liquid dimethyl ether from 227 to 343 K. *J. Chem. Eng. Data* **2003**, *48*, 426−429.
(5) Wu, J. T.; Liu, Z. G.; Jin, X. G.; Pan, J. The thermal conductivity of some oxygenated fuels and additives in the saturated liquid phase. *J. Chem. Eng. Data* **2005**, *50*, 102−104.
(6) Wu, J. T. Development of the new thermophysical properties measurement system and research of thermophysical properties of dimethyl ether. Ph.D. Dissertation, Xi'an Jiaotong University, Xi'an, 2003.
(7) Carslaw, H. S.; Jaeger, J. C. *Conduction of Heat in Solids*, 2nd ed.; Oxford University Press: London, 1959.
(8) Wakeham, W. A.; Nagashima, A.; Sengers, J. V. *Experimental Thermodynamics Vol. III, Measurement of the Transport Properties of Fluids*; Blackwell Scientific Publications: Oxford, 1991.

(9) Healy, J. J.; De Groot, J. J.; Kestin, J. The theory of the transient hot-wire method for measuring thermal conductivity. *Physica C* **1976**, *82*, 392−408.
(10) Wang, Y. G. Experimental research of thermal conductivity of liquid using transient two hot-wires method. Ph.D. Dissertation, Xi'an Jiaotong University, Xi'an, 2005.
(11) Wu, J. T.; Liu, Z. G.; Pan, J. Development of fluid thermophysical property measurement system with high Accuracy. *J. Xi'an Jiaotong Univ.* **2004**, *38*, 937−942.
(12) Ramires, M. L. V.; Nieto de Castro, C. A. Uncertainty and performance of *the* transient hot wire method. In *Proceedings of the Eighth International Symposium on Temperature and Thermal Measurements in Industry and Science, TEMPMEKO 2001*, Berlin, June 19−21, 2001; VDE VERLAGGMBH: 2002; Vol. 2, pp 1181−1185.
(13) Lemmon, E. W.; McLinden, M. O.; Huber, M. L. *Reference Fluid Thermodynamic and Transport Properties, NIST Standard Reference Database 23* (*REFPROP*), version7.0; National Institute of Standard and Technology: Boulder, CO, 2003.

Received for review August 3, 2005. Accepted September 29, 2005. This work has been supported by the National Science Foundation of China (Grants 50306021 and 50336020) and the National Basic Research Priorities Program of Ministry of Science and Technology of China (Grant 2001CB209208).

JE050305Z